Magnetic anisotropy of Sm_2Fe_{17} single crystals

L. V. B. Diop,[1,*] M. D. Kuz'min,[2] K. P. Skokov,[1] D. Yu. Karpenkov,[1] and O. Gutfleisch[1]
[1]*Institut für Materialwissenschaft, Technische Universität Darmstadt, D-64287 Darmstadt, Germany*
[2]*Aix-Marseille Université, IM2NP, Faculté St. Jérôme, F-13397 Marseille, Cedex 20, France*
(Received 19 April 2016; revised manuscript received 13 June 2016; published 12 October 2016)

The previously accepted notion that the spontaneous magnetization of Sm_2Fe_{17} lies in the basal plane of the crystal is true only approximately, and then only around room temperature. At low temperatures the magnetization, whose orientation is not fixed by the symmetry, is found to deviate from the basal plane by as much as 10°. The threefold symmetry axis is a hard direction; to magnetize the crystal in this direction, a magnetic field of about 9 T is required. The hard-axis magnetization arrives at saturation discontinuously, by way of a first-order phase transition. The behavior is a general one for trigonal ferromagnets where $K_1 < 0$ and the leading trigonal anisotropy constant is nonzero, $K_2' \neq 0$. Although of universal occurrence, the first-order transition is only visible at low temperatures, where it is accompanied by a magnetization anomaly of sufficient size.

DOI: 10.1103/PhysRevB.94.144413

I. INTRODUCTION

The binary system Sm_2Fe_{17} attracted much attention in the past. The interest was mainly due to its nitride, $Sm_2Fe_{17}N_3$ [1–11], which in the decade of the 1990s was regarded as a promising permanent magnet material, a potential successor to $Nd_2Fe_{14}B$. At the heart of that vast research activity was the process of interstitial nitrogenation [2–4], turning the weak easy-plane anisotropy of Sm_2Fe_{17} into an outstandingly strong easy-axis anisotropy of $Sm_2Fe_{17}N_3$ and at the same time boosting the Curie temperature by as much as ∼360 K. For a detailed study of the anisotropy transformation, it was necessary to compare the anisotropies of the nitride and of the parent compound. However, the latter proved remarkably elusive. Despite the extraordinary research effort and accordingly extensive literature, we are unaware of any single-crystal study of pure Sm_2Fe_{17}. The true easy direction, the anisotropy constants, and the related properties remain unknown. The accepted opinion of Sm_2Fe_{17} as an easy-plane ferromagnet corresponds to reality only approximately, and then only around room temperature. In fact, the orientation of the spontaneous magnetization in Sm_2Fe_{17} is not fixed by the symmetry and has been unknown so far. One interesting effect found in an earlier study of oriented Sm_2Fe_{17} powder [25] is a first-order phase transition induced by a magnetic field applied along the threefold axis [001], which is a hard direction. This transition was also observed in pseudobinary single crystals of composition $Sm_2(Fe_{1-x}Al_x)_{17}$ [12]. For a systematic study of the magnetic anisotropy, we set out to grow single crystals of pure Sm_2Fe_{17}. This study is reported in the subsequent sections, which are organized as follows. Section II describes briefly the experimental techniques and Sec. III presents the results of the measurements. The theoretical model is introduced in Sec. IV. This is followed by a discussion (Sec. V) and a summary (Sec. VI).

II. EXPERIMENTAL DETAILS

The rhombohedral Sm_2Fe_{17} phase forms by the peritectic reaction $L + \gamma\text{-Fe} \xrightarrow{1553\,K} Sm_2Fe_{17}$. This means that directly after melting, it is mostly α-Fe and Sm-rich phases that are present in the as-cast ingots and, in order to achieve an almost single-phase state, a long heat treatment at temperatures above 1273 K is required. We found that stoichiometric Sm_2Fe_{17} ingots, even after being annealed for one to two months at 1323 K, still contained α-Fe inclusions, and the average grain size was no more than $50-100\,\mu$m. This does not suffice for a proper measurement of magnetic anisotropy. We found it advantageous to start from a slightly off-stoichiometric composition and to have a small amount of liquid Sm-rich phase between the grains during the annealing. In this case, the grain growth proceeded more rapidly, and no α-Fe was present in the sample. Thus, by changing the stoichiometry of the master alloy from Sm_2Fe_{17} to $SmFe_7$, grains of rhombohedral Sm_2Fe_{17} as large as 1 to 2 mm were obtained after annealing the ingot for several weeks at temperatures above 1273 K. An energy-dispersive x-ray spectroscopy (EDS) analysis revealed for the grains a final composition of $Sm_2Fe_{16.97}$, while excess samarium was found in the intergranular space.

The starting $SmFe_7$ alloy was prepared by melting high-purity elements (Sm: 99.9%; Fe: 99.99%) in an induction furnace under a purified atmosphere of argon. The resulting ingot was sealed in an evacuated quartz tube and annealed in a resistive furnace as follows. It was heated up to 1373 K at a rate of 5 K/h. Then, it was slowly cooled down to 1273 K during 21 days, kept at this temperature for 10 days, and subsequently quenched in water. Several 1–2 mm-large grains were extracted and checked for single crystallinity. The best one of them was selected for magnetic measurements and oriented by back-scattering Laue x-ray diffraction. The crystal structure of Sm_2Fe_{17} is well established; it crystallizes in the rhombohedral Th_2Zn_{17}-type structure (space group $R\bar{3}m$). The unit cell parameters determined by means of powder diffraction ($a = 8.551$ Å and $c = 12.449$ Å) are in good agreement with earlier reported studies. Temperature and field dependence of the magnetization was measured on the oriented crystal in static magnetic fields up to 14 T

*diop@fm.tu-darmstadt.de

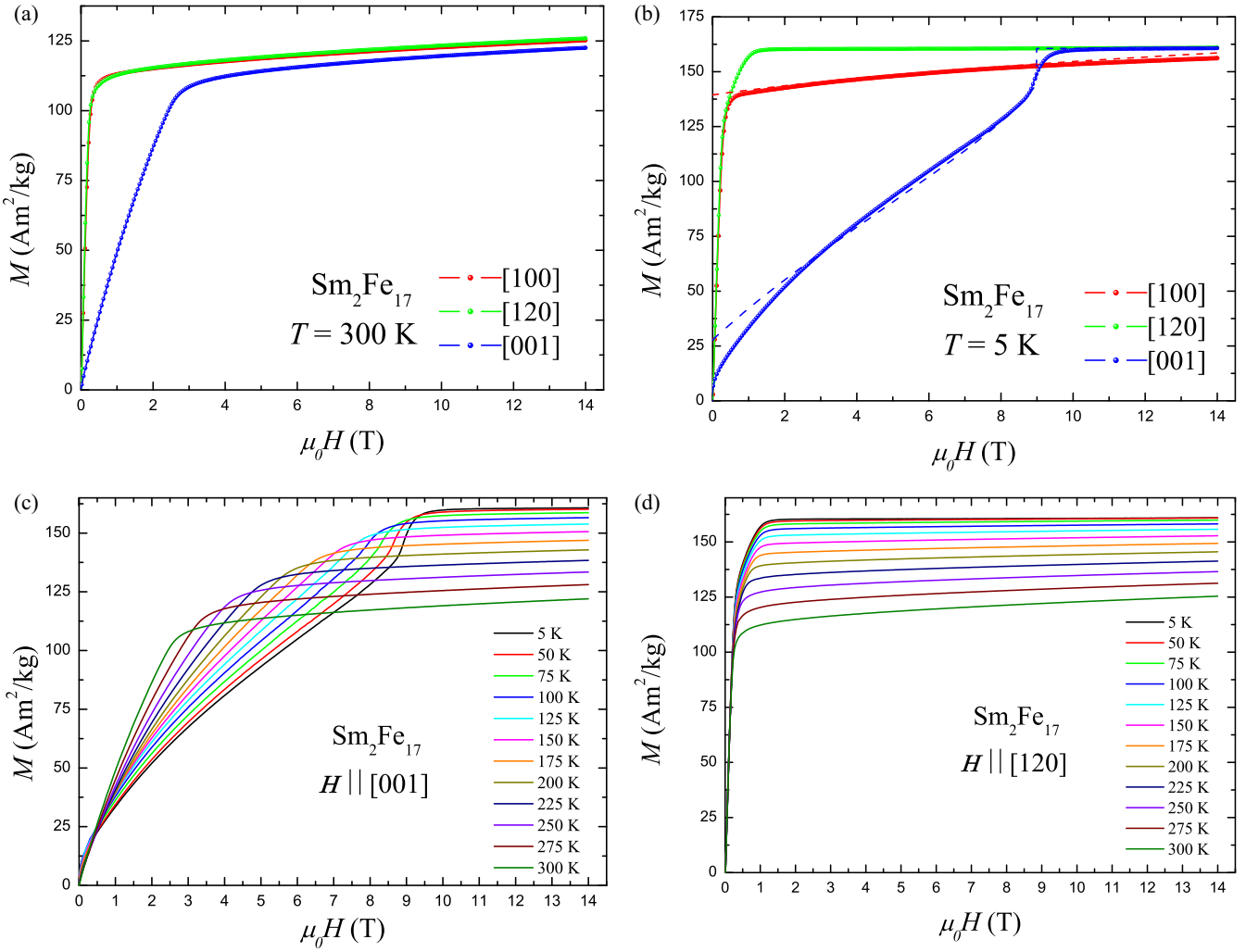

FIG. 1. Magnetization curves of Sm_2Fe_{17} measured along the principal axes at (a) $T = 300$ K and (b) $T = 5$ K. Temperature evolution of the magnetization curves along the (c) [001] axis and (d) [120] axis of Sm_2Fe_{17}.

at temperatures between 5 and 450 K using a commercial magnetometer (Quantum Design PPMS-14).

III. RESULTS

Figure 1(a) displays the magnetization curves of Sm_2Fe_{17} measured along the principal crystallographic directions at 300 K. Typical behavior of easy-plane magnetocrystalline anisotropy is observed; the data measured along the threefold symmetry axis [001] clearly identifies this as the hard magnetization direction. The two curves recorded along [100] and [120] directions are practically identical, reflecting a weak magnetic anisotropy within the basal plane for this system at room temperature. The anisotropy field, $\mu_0 H_a$, determined from the kink in the magnetic hard-axis curve amounts to 2.8 T at 300 K. Another noteworthy observation is the anisotropy of the magnetic moment, i.e., the hard-axis magnetization curve does not fully approach the easy-axis one above $\mu_0 H_a$. The magnetization along the hard axis is 3% smaller than that along the easy axis, even in an applied magnetic field of 14 T.

At 5 K [see Fig. 1(b)], a strong magnetic anisotropy is present within the basal plane, as can be seen from the marked difference between the magnetization curves along the [100] and [120] directions. The ratio of the spontaneous magnetizations along the [100] and [120] directions becomes nearly equal to $0.868 \approx \cos(\pi/6)$, which confirms good crystal quality and orientation. Furthermore, the magnetization curve measured along the threefold symmetry axis exhibits a first-order spin-reorientation transition at a critical field $\mu_0 H_{cr}$ of about 9 T. Such magnetic field-induced phase transitions are often called first-order magnetization process (FOMP) [13]. The magnetization along [001] axis is saturated above $\approx$9.5 T; therefore, the observed FOMP is of type I, following the nomenclature of Asti and Bolzoni [13]. Moreover, the spontaneous magnetization has nonzero projection on the hard direction, reflecting the deviation of the easy directions from the basal plane.

Figure 1(c) presents the temperature evolution of the magnetization curves of Sm_2Fe_{17} along the hard axis. It follows from these measurements that the magnetic behavior in Sm_2Fe_{17} is rather complex. The low-temperature magnetization data reveal the presence of a FOMP at about 9 T. One can see in Fig. 1(c) that both the critical field of the FOMP and the magnetic anisotropy field decrease monotonically upon

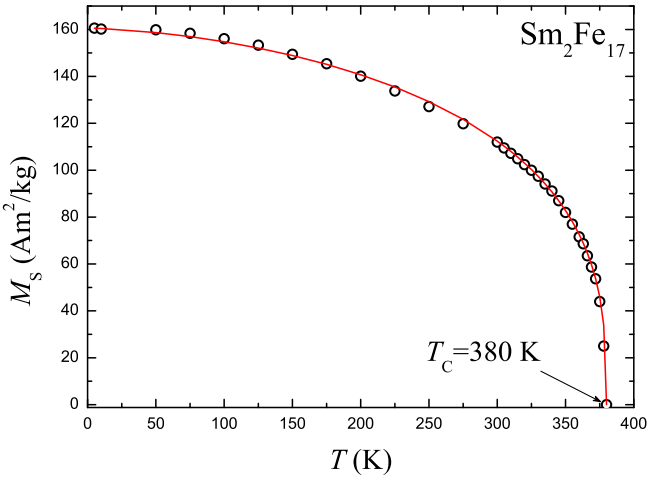

FIG. 2. Spontaneous magnetization of Sm_2Fe_{17} as a function of temperature.

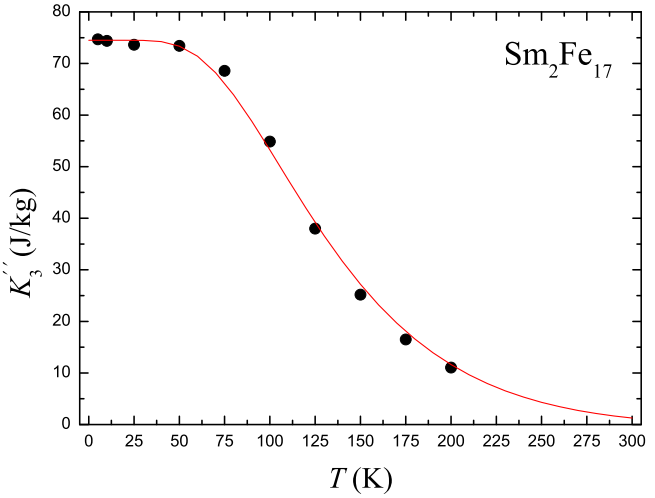

FIG. 3. Temperature dependence of the anisotropy constant K_3''.

heating. As temperature increases, the FOMP smears out gradually, becoming imperceptible above 100 K. The angle δ_0 between the easy direction and the basal plane, determined from the initial part of the magnetization curve along the hard axis, decreases with temperature and becomes indiscernible above 250 K.

The isothermal magnetization curves of Sm_2Fe_{17} taken along the [120] direction at several fixed temperatures between 5 K and 300 K are illustrated in Fig. 1(d). The magnetization saturates at low field following steep initial increase. The slope of the initial linear sections is independent of temperature and determined by the demagnetizing factor. The spontaneous magnetization M_S was deduced from the magnetization curves along [120] axis by linear extrapolation to zero internal field and is estimated to be 161 A m^2/kg at $T = 5$ K. Above room temperature, M_S was obtained from Arrott-Belov plots [14,15]. The spontaneous magnetization of Sm_2Fe_{17} is plotted against temperature in Fig. 2. The solid line is a fit to the following expression [16]:

$$M_S(T) = M_S(0)\left[1 - s\left(\frac{T}{T_C}\right)^{\frac{3}{2}} - (1-s)\left(\frac{T}{T_C}\right)^{5/2}\right]^{1/3}, \quad (1)$$

with $M_S(0) = 161$ A m^2/kg, $T_C = 380$ K, and $s = 0.7$. Such a shape of $M_S(T)$, with $s = 0.7$, is typical for Fe-based intermetallic ferromagnets [16,17].

The anisotropy constant K_3'', defined by Eq. (2) below, was determined as one-half of the area between the magnetization curves along [120] and [100] measured at the same temperature. The corresponding temperature dependence of K_3'' is presented in Fig. 3. The in-plane anisotropy decreases rapidly with T and becomes negligible towards room temperature.

IV. THEORY

A. The model

We adopt a one-sublattice approximation for Sm_2Fe_{17}. The magnetic moments of Sm and Fe are aligned by a strong exchange interaction ($B_{ex} = 380$ T [10]) so that the angle between them is small ($\sim 2^\circ$) and can be neglected. Therefore, in the following analysis Sm_2Fe_{17} is regarded as a simple ferromagnet. For simplicity, we shall first limit ourselves to $T = 0$ and postulate that the magnetization vector does not change its magnitude as it rotates, $|\boldsymbol{M}| = M_0 = \text{const}$. The magnetization process can then be described by means of a simple expression for the energy of the system, consisting of its anisotropy energy and a Zeeman term:

$$\begin{aligned} E = {} & K_1 \sin^2\theta + K_2 \sin^4\theta + K_2' \sin^3\theta \cos\theta \sin 3\varphi \\ & + K_3 \sin^6\theta + K_3' \sin^3\theta \cos\theta (11\cos^2\theta - 3)\sin 3\varphi \\ & + K_3'' \sin^6\theta \cos 6\varphi - \mu_0 \boldsymbol{H} \cdot \boldsymbol{M}. \end{aligned} \quad (2)$$

Equation (2) complies with the point symmetry group D_{3d} ($\bar{3}m$) and is limited to sixth-order terms. According to the International Tables for Crystallography [19], the z (hexagonal c) axis is set along the threefold symmetry axis and the x (a) axis is parallel to a twofold axis, as in Fig. 4. (In theory literature, one often finds a different setting of the x axis, whereby it lies in one of the mirror planes [20]; in that case, $\sin 3\varphi$ in Eq. (2) should be replaced with $\cos 3\varphi$.)

B. Orientation of spontaneous magnetization

We begin the analysis of Eq. (2) by considering a special case of $H = 0$. Since the sixth-order Stevens factor of samarium is zero, the sixth-order anisotropy terms—those in K_3, K_3', and K_3''—are expected to be small and will be omitted from Eq. (2).

The leading anisotropy constant, K_1, is negative because z is a hard axis. The second anisotropy constant, K_2, will be neglected in the subsequent analysis. The reason is that a nonzero K_2 does not qualitatively change any of the conclusions reached in the simplified model with $K_2 = 0$. Moreover, the magnetization curve along the z axis is fitted best with $K_2 = 0$. The other fourth-order anisotropy constant, K_2', is peculiar to the trigonal symmetry. It will turn out to play a central role in the model.

Our model is distinct from the one used previously [21] to interpret a FOMP in an isostructural compound $Nd_2Fe_{14}Si_3$. In Ref. [21], also, Eq. (2) was taken for a starting point;

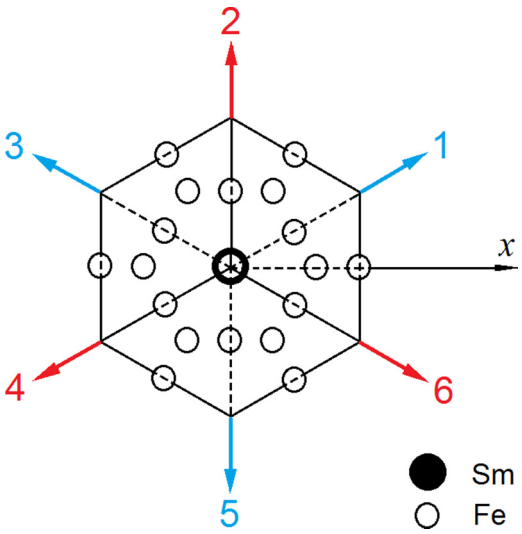

FIG. 4. Top view of the rhombohedral unit cell of Sm_2Fe_{17} with six easy directions. The x axis (hexagonal a) lies in the plane of the drawing, while the z axis points out of the plane, passing through the center.

however, all but the first two anisotropy constants were set to zero. The trigonality of $Nd_2Fe_{14}Si_3$ was thus neglected, and the calculations (Fig. 9 of Ref. [21]) failed to reproduce the magnetization projection on the hard axis, characteristic of trigonal ferromagnets.

Upon division by $|K_1|$, Eq. (2) becomes

$$E' = -\sin^2\theta \pm \kappa \sin^3\theta \cos\theta \sin 3\varphi, \tag{3}$$

where

$$E' = E/|K_1| \tag{4}$$

and

$$\kappa = |K_2'|/|K_1|. \tag{5}$$

Thus, by definition, κ is a positive quantity.

The orientation of easy directions is sought by minimizing E' with respect to θ and φ. The trivial solutions, $\theta = 0$ and $\theta = \pi$, can be excluded *a priori* since these are known to correspond to hard directions (maxima of E'). The minimization with respect to φ yields six possible azimuthal orientations,

$$\varphi_n = -\pi/6 + n\pi/3, \quad n = 1,2,\ldots,6. \tag{6}$$

Setting these values into the necessary condition of a minimum of E' with respect to θ results in

$$\pm\kappa = \frac{2(-1)^n \cos\theta}{\sin\theta(1 - 4\cos^2\theta)}. \tag{7}$$

It will be recalled that κ is an essentially positive quantity, the $\pm$ signs in Eqs. (3) and (7) being equal to the sign of K_2'.

The six values of the polar angle corresponding to the easy directions are given by

$$\theta_n = \pi/2 \mp (-1)^n \delta_0, \quad n = 1,2,\ldots,6, \tag{8}$$

where δ_0 is an acute angle satisfying the following equation,

$$\kappa = \frac{2\tan\delta_0}{1 - 4\sin^2\delta_0}. \tag{9}$$

Like κ, δ_0 is a positive quantity, $0 < \delta_0 < \pi/6$. It describes the deviation of the easy direction from the basal plane. The angle δ_0 is a single parameter characterizing the peculiar noncoplanar shape of the asterisk of easy axes. In the following sections, it will become apparent that δ_0 (or alternatively κ) is also a sole parameter governing the shape of the magnetization curves. Equation (9) provides a one-to-one relation between both parameters.

While κ (or δ_0) characterizes the degree of noncoplanarity of the easy asterisk, the sign of K_2' determines its orientation in relation to the rhombohedral unit cell (see Fig. 4). There are two possibilities in this respect.

(1) $K_2' < 0$, which are the lower signs in Eqs. (3), (7), and (8). The easy directions corresponding to n odd numbers deviate from the basal plane upwards, tending towards the invisible (dashed) edges of the cell. At the same time, the easy directions with even numbers deviate by the same amount downwards from the basal plane, to become nearly parallel to the visible (solid) edges of the rhombohedron. One can speak in this case of [100]-like easy axes, in the sense of their proximity to the edges of the rhombohedral cell.

(2) $K_2' > 0$, which are the upper signs in Eqs. (3), (7), and (8). The odd-numbered easy directions deviate downwards, while those with even numbers deviate upwards. The easy asterisk is turned through $\pi/3$ with respect to its orientation in the previous case. The easy axes now tend towards the *secondary* body diagonals of the rhombohedron—they are [111]-like. (The main body diagonal does not count; it is a hard direction.)

Thus, the magnitude of K_2' (in relation to that of K_1) determines the degree of noncoplanarity of the easy asterisk, as described by the angle δ_0. The sense of the noncoplanarity—either [100]- or [111]-like—is determined by the sign of K_2'. This sign is unknown at present, and it cannot be found from the magnetization curves presented in Fig. 1.

C. Magnetization curves: $H \parallel [001]$

Let the applied magnetic field be nonzero and point in the *positive* z direction. Equation (2), with $K_2 = K_3 = K_3' = K_3'' = 0$, then becomes

$$E = K_1 \sin^2\theta + K_2' \sin^3\theta \cos\theta \sin 3\varphi - \mu_0 H M_0 \cos\theta. \tag{10}$$

Minimization with respect to φ—on condition of θ being acute—yields

$$\varphi_0 = -(\pi/6)\,\mathrm{sign}\, K_2',$$

or, equivalently, $\varphi_0 + 2\pi/3$ or $\varphi_0 + 4\pi/3$. In either case,

$$\min_{\varphi}(K_2' \sin 3\varphi) = -|K_2'|.$$

Substituting $-|K_2'|$ for $K_2' \sin 3\varphi$ in Eq. (10) and dividing the result by $|K_1|$, we obtain

$$E' = -\sin^2\theta - \kappa \sin^3\theta \cos\theta - h\cos\theta, \tag{11}$$

where h is a dimensionless magnetic field,

$$h = \frac{\mu_0 H M_0}{|K_1|}, \tag{12}$$

and E' and κ are as defined above [see Eqs. (4) and (5)]. The necessary condition of a minimum of $E'(\theta)$ is

$$h\sin\theta = 2\sin\theta\cos\theta + \kappa\sin^2\theta(4\cos^2\theta - 1), \quad (13)$$

whence either $\theta = 0$ or

$$h = 2\cos\theta + \kappa\sin\theta(4\cos^2\theta - 1). \quad (14)$$

A third solution, $\theta = \pi$, can be discarded at this stage since it obviously corresponds to a maximum of $E'(\theta)$.

The trivial solution, $\theta = 0$, pertains to a saturated state where $M \parallel H$. This state is stable if H is sufficiently large.

The nontrivial solution (14) describes the process of magnetization rotation in weaker fields. It is convenient to rewrite Eq. (14) in terms of reduces magnetization in the z direction, $m = \cos\theta$,

$$h = 2m + \kappa(4m^2 - 1)\sqrt{1 - m^2}. \quad (15)$$

The most peculiar part of this expression is the second term, plotted in Fig. 5(a) (solid line). It features a minimum at $m = 0$, a change of sign at $m = \frac{1}{2}$, a maximum at $m = \frac{1}{2}\sqrt{3}$, and a very steep descent to zero at $m = 1$. The negative of the second term is also shown in Fig. 5(a) (dashed line); both curves are readily recognized as parts of the well-known Lissajous curve for the frequency ratio 1:3.

The first term in Eq. (15) puts these features on a linearly growing background, as shown in Fig. 5(b). The parameter κ ($\kappa > 0$) controls the relative weight of the second term in Eq. (15) and therefore the shape of the entire magnetization curve. The smaller κ, the narrower the interval of negative h on the left and the falling part on the right. However, neither of these two features will disappear completely at any finite κ. In particular, the negative slope on the right will survive: The negative derivative due to the second term in Eq. (15) tends to $-\infty$ as $m \to 1$ and prevails over the finite positive slope contributed by the first term.

We finally turn to the more usual presentation of the magnetization curve as m vs h and discard its unphysical part lying in the second quadrant [see Fig. 5(c)]. The following conclusions can be drawn.

(1) The shape of the magnetization curve is uniquely determined by the parameter κ [or by the angle δ_0, which is uniquely related to κ through Eq. (9)]. In particular, the initial magnetization along z equals $\sin\delta_0$. For small κ, $\sin\delta_0 \approx \kappa/2$. Thus, a nonzero offset magnetization will remain present as long as $\kappa \neq 0$.

(2) On approach to saturation, there is a zone of instability, where $\partial m/\partial h < 0$. This zone is overcome by way of a first-order transition accompanied by a step-wise magnetization growth to saturation (a FOMP of type I according to Asti and Bolzoni [13]). The smaller κ, the smaller the jump in the magnetization curve. However, the jump will remain present for any finite κ. Moreover, the FOMP will not be destroyed if a nonzero K_2 and/or six-order anisotropy constants are allowed for. The presence of a FOMP in the magnetization curve along the (hard) threefold axis is thus a characteristic of trigonal ferromagnets. It is due to their symmetry and is not contingent upon any special relation among the anisotropy constants. In this respect, the FOMP under examination here is distinct from that in uniaxial magnets, earlier studied by Onopriyenko

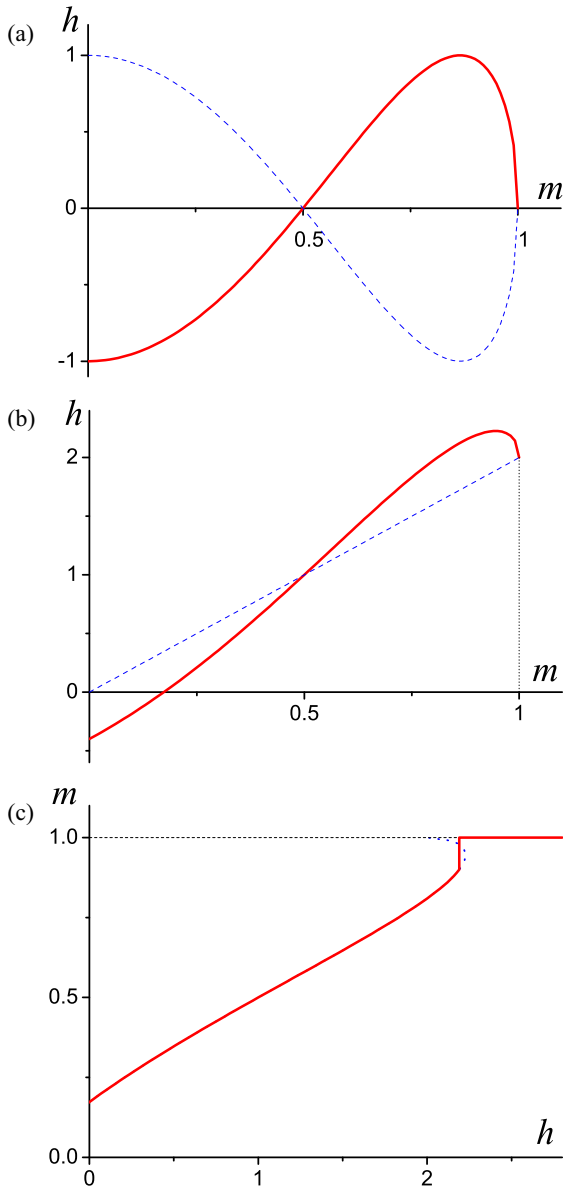

FIG. 5. Construction of the magnetization curve along the c axis: (a) the second term of Eq. (15) with $\kappa = 1$ (solid line) and its negative (dashed); (b) the complete Eq. (15) with $\kappa = 0.4$ (solid line) and its first term alone (dashed); (c) the same as (b) but presented as m vs h.

[22] (see also Melville *et al.* [23], Asti and Bolzoni [13], and Asti [24]). In the uniaxial case, both the sign and the magnitude of the second anisotropy constant K_2 are essential for a FOMP to occur. By contrast, neither the sign nor the magnitude of K_2', nor even the presence of a nonzero K_2, matter for the occurrence of the indestructible FOMP in a trigonal magnet. The only way to get rid of the FOMP is to renounce the trigonality altogether by setting $K_2' = 0$ ($\kappa = 0$). One is compelled to conclude that this FOMP is a general property of trigonal magnets, which they owe to their symmetry.

For a quantitative description of the FOMP, one should equate the energies of the phases on both sides of the first-order transition, as given by Eq. (11) with $\theta = 0$ and $\theta = \theta_{cr}$. This results in a relation between the critical field and the critical

angle:

$$h_{cr} = (1 + \cos\theta_{cr})(1 + \kappa \sin\theta_{cr}\cos\theta_{cr}). \quad (16)$$

At the same time, the angled phase must satisfy the equilibrium condition, i.e., Eq. (14) with $h = h_{cr}$ and $\theta = \theta_{cr}$. Eliminating h_{cr} from the conjunction of both equations, one obtains a relation between the critical angle and the main model parameter κ:

$$\kappa = \frac{1 - \cos\theta_{cr}}{\sin\theta_{cr}} \frac{1}{3\cos^2\theta_{cr} - \cos\theta_{cr} - 1}. \quad (17)$$

This can be conveniently rewritten directly in terms of the critical magnetization, $m_{cr} = \cos\theta_{cr}$:

$$\kappa = \sqrt{\frac{1 - m_{cr}}{1 + m_{cr}}} \frac{1}{3m_{cr}^2 - m_{cr} - 1}. \quad (18)$$

D. Magnetization curves: $H \parallel [100]$

In this case the relative strengths of the anisotropy terms in Eq. (2) are rather different. The magnetization vector is very close to the basal plane, the angle θ tending to $\pi/2$ as the field grows. In a good approximation, one can simply set $\theta = \pi/2$, making the terms in K_2' and K_3' vanish. The axial (nonprimed) terms are now constant and can be neglected. The energy expression takes a simple form,

$$E = K_3'' \cos 6\varphi - \mu_0 H M_0 \cos\varphi. \quad (19)$$

The minimization with respect to φ is straightforward and leads to a result known for hexagonal magnets,

$$h = m(4m^2 - 1)(4m^2 - 3). \quad (20)$$

Here, m stands for reduced magnetization, $m = \cos\varphi$, and h is reduced magnetic field,

$$h = \frac{\mu_0 H M_0}{12K''_3}. \quad (21)$$

V. DISCUSSION

The experimental results presented in Sec. III reveal that the magnetic behavior of Sm_2Fe_{17} is most interesting at low temperature and in a magnetic field parallel to the threefold axis [001] [see Fig. 1(b)]. According to our data, at zero field the magnetization has a nonzero projection on the [001] direction. Then a progressive growth of the magnetization occurs. A further steplike rise at about 9 T brings the magnetization to saturation at $M_0 = 161\,\mathrm{A\,m^2/kg}$.

Taking from our experiment $m_{cr} \approx 0.9$, we find by means of Eq. (18) that $\kappa \approx 0.4$. This corresponds to $\delta_0 \approx 10^\circ$, cf. Eq. (9). Such values of κ and δ_0 are not unusual. According to Eq. (9), the theoretical upper bound for δ_0 is 30°, and a value as high as 26° was observed in an isostructural compound Pr_2Co_{17} [26,27], corresponding to $\kappa = 4.2$. On the other hand, a smaller δ_0 was found in Nd_2Co_{17}, $\delta_0 = 7.5^\circ$ [26,27], which corresponds to $\kappa = 0.28$. At any rate, the conclusion made in Ref. [12]—that $\delta_0 = 0$ for pure Sm_2Fe_{17}—is a mistake. It was too rash to extrapolate to $x = 0$ the dependence $\delta_0(x)$ obtained for $Sm_2(Fe_{1-x}Al_x)_{17}$ between $x = 0.075$ and $x = 0.145$ only.

Turning back to our model, we obtain from Eq. (16) with $\cos\theta_{cr} = m_{cr} = 0.9$ and $\kappa = 0.4$,

$$h_{cr} = 2.2. \quad (22)$$

Contrasting this value with the experimental critical field at $T = 5\,\mathrm{K}$, $\mu_0 H_{cr} = 9.0\,\mathrm{T}$ [Fig. 1(b)], we obtain 4.1 T for the conversion factor between the dimensionless field h and the usual field in teslas. Now the theoretical magnetization curve of Fig. 5(c) can be rescaled and presented together with the experimental data [see Fig. 1(b) (dashed curve)]. The vertical scaling factor equals the saturation magnetization, M_0. Finally, setting into Eq. (12) $h = h_{cr} = 2.2$, $H = H_{cr} = 9.0\,\mathrm{T}$, and $M_0 = 161\,\mathrm{A\,m^2/kg}$, we get

$$K_1 = -660\,\mathrm{J/kg} \quad (23)$$

and

$$|K_2'| = \kappa|K_1| = 260\,\mathrm{J/kg}. \quad (24)$$

The sign of K_2' cannot be determined from our data.

The anisotropy constants K_2 and K_3 are apparently so small that they cannot be deduced from our data. They were set to zero, initially in order to simplify the model. Our subsequent attempts to improve the fit shown in Fig. 1(b) by allowing for $K_2 \neq 0$ proved unsuccessful. If anything, a nonzero K_2 made the agreement with experiment worse. Therefore, $K_2 = 0$ was left as the best-fit value. Some improvement in the middle of the [001] curve in Fig. 1(b) (at fields around 5 T) could be achieved by assuming a small nonzero K_3' ($|K_3'| \sim 10\,\mathrm{J/kg}$) *of the same sign as* K_2'. We did not pursue this route further because the effect was small and did not help to improve the initial part of the curve, below 2 T, where the agreement with experiment is conspicuously poor. At this point, we are inclined to ascribe the disagreement to magnetic domains, which are not taken into account by the model.

Let us now turn to the anisotropy constant K_3''. The values plotted against temperature in Fig. 3 (dark circles) were deduced directly from the experimental curves, as explained in Sec. III. The solid line in Fig. 3 is a fit to the following expression,

$$K_3''(T) = \frac{K''_3(0)}{0.0384} B_{5/2}^{(5)}\left(\frac{25}{7}\frac{\mu_B B_{ex}}{kT}\right). \quad (25)$$

Here $K_3''(0) = 75\,\mathrm{J/kg}$ is the low-temperature limit. In fact, this value is just the ordinate of the left-most data point, whose abscissa is $T = 5\,\mathrm{K}$. The symbol $B_{5/2}^{(5)}(x)$ stands for the generalized Brillouin function [28] of order 5 for $J = 5/2$, as appropriate for Sm^{3+}; the numerical constant 0.0384 serves to normalize the function to unity at $T = 0$. The argument of the generalized Brillouin function contains the exchange field on Sm, B_{ex}, which is a temperature-dependent quantity that falls off with temperature proportionally to the spontaneous magnetization. So the expression on the right-hand side of Eq. (25) was used to compute $B_{ex}(T)$, whose low-temperature limit, $B_{ex}(0)$, was the only adjustable parameter in the entire procedure. We found $B_{ex}(0) = 315\,\mathrm{T}$ to be the best-fit value. This is about 20% less than the value deduced from the observation of intermultiplet transitions in an inelastic neutron scattering experiment [10], $B_{ex} = 380\,\mathrm{T}$.

One may find it strange that temperature dependence of K_3'', a sixth-order anisotropy constant, is given by the fifth-order generalized Brillouin function and not by the sixth-order one, as stipulated by the linear theory [28]. The reason is that the ground multiplet of samarium has a rather small angular momentum, $J = 5/2$, and so the main, intramultiplet contribution to the sixth-order anisotropy vanishes because the triangle rule ($n \leqslant 2J$) is not fulfilled for $n = 6$. In the next approximation, as the first excited multiplet is taken into account (J-mixing), two extra contributions to K_3'' arise, in $B_{5/2}^{(5)}(x)$ and in $B_{5/2}^{(7)}(x)$ [29,30]. The latter is nil for Sm, on account of the same triangle rule: $B_{5/2}^{(7)}(x) \equiv 0$. Therefore, the first nonvanishing contribution to K_3'' is the one in $B_{5/2}^{(5)}(x)$.

It would be instructing to compare our set of anisotropy constants ($T = 5\,\mathrm{K}$),

$$K_1 = -660\,\mathrm{J/kg}, \quad |K_2'| = 260\,\mathrm{J/kg},$$
$$K''_3 = 75\,\mathrm{J/kg}, \quad K_2 = K_3 = K_3' = 0,$$

with earlier data obtained on polycrystalline samples. Unfortunately, the possibilities for such a comparison are rather limited because Sm_2Fe_{17} is not particularly suitable for making oriented powder samples. One finds in the literature a K_1 that is 1.7 times too small ($K_1 = -381\,\mathrm{J/kg}$ [18], $T = 4.2\,\mathrm{K}$); this should not be viewed as unreasonable. No information is available on the other anisotropy constants. As regards other magnetic characteristics of Sm_2Fe_{17}, they are in fair agreement with the literature. Thus, our Curie temperature and saturation magnetization, $T_C = 380\,\mathrm{K}$ and $M_0 = 161\,\mathrm{A\,m^2/kg}$, compare well to those found in polycrystalline samples, $T_C = 385\,\mathrm{K}$ [18] and $M_0 = 165\,\mathrm{A\,m^2/kg}$ [31]. For the critical field of the FOMP, we find a value of 9 T, as against 11.2 T obtained on oriented powder [25].

To complete the picture, one also needs a theoretical magnetization curve with the magnetic field being parallel to a hard direction in the basal plane, i.e., $\boldsymbol{H}||[100]$. The calculated magnetization curve is shown in Fig. 1(b) (dashed line). The values of the parameters used in the calculation were as previously determined from the experiment: $K_3'' = 75\,\mathrm{J/kg}$ at $T = 5\,\mathrm{K}$ (see Fig. 3) and $M_0 = 161\,\mathrm{A\,m^2/kg}$. Thus, $h = 1$ corresponds to about 5.6 T. Comparing the experimental and calculated [100] curves, one observes that the former is well reproduced by the calculations.

Turning to the room-temperature data, we note a significant moment anisotropy: The hard-axis magnetization does not become quite as high as the easy-axis one, even above the anisotropy field. A finite gap between the two curves persists up to the highest available field, 14 T. Magnetization anisotropy was predicted by Callen and Callen [32,33] and observed in various intermetallic systems. In Sm_2Fe_{17}, the difference is not particularly large, $3.5\,\mathrm{A\,m^2/kg}$ or 3% at room temperature. For comparison, in La_2Co_7 it is as high as 10% at room temperature [34].

Finally, our model predicts a compulsory FOMP in a magnetic field $\boldsymbol{H} \parallel [001]$ for all trigonal magnets where [001] is a hard direction. Reference [25] confirms this prediction for Pr_2Fe_{17} and Nd_2Fe_{17}. However, no FOMPs were observed in either Pr_2Co_{17} or Nd_2Co_{17} single crystals [27]. It should be noted though, that in the high-field experiments of Ref. [27], magnetization was measured once every 5 tesla, so having missed a FOMP cannot be ruled out at present. A more careful measurement is highly desirable.

VI. SUMMARY

The low-temperature magnetic structure of Sm_2Fe_{17} can be described as a noncoplanar easy asterisk. There are six equivalent easy directions close to the [120] axes but deviating from the basal plane by $\pm 10^\circ$ (at $T = 5\,\mathrm{K}$). The threefold symmetry axis [001] is a hard magnetization direction.

The magnetization behavior can be described by a simple model. The magnetization process along [100] is governed by a single anisotropy constant and proceeds in a similar fashion as in hexagonal magnets. Of most interest is the magnetization process in the hard direction [001], where the trigonality of Sm_2Fe_{17} comes to the fore. The main feature of this process is the presence of an indestructible symmetry FOMP, which takes place regardless of the values of model parameters. In the simplest approach, the process can be presented as interplay of just two anisotropy terms, the ratio of the corresponding anisotropy constants κ being the sole parameter of the model. This parameter determines the shape of the [001] magnetization curve, in particular, the heights of the initial offset and of the final jump associated with the FOMP. As κ decreases, the height of the FOMP tends to zero asymptotically. The magnetization will stay discontinuous—the FOMP will not turn into a second-order phase transition—as long as the crystal remains essentially trigonal ($\kappa \neq 0$).

ACKNOWLEDGMENTS

The financial support by the German federal state of Hessen through its excellence programme LOEWE "RESPONSE" is acknowledged.

[1] T. Iriyama, K. Kobayashi, and H. Imai, Magnetic materials containing rare earth element iron nitrogen and hydrogen, European Patent Application EP0369097 A1, May 23, 1990.

[2] J. M. D. Coey and H. Sun, J. Magn. Magn. Mater. **87**, L251 (1990).

[3] H. Sun, J. M. D. Coey, Y. Otani, and D. P. F. Hurley, J. Phys.: Condens. Matter **2**, 6465 (1990).

[4] Y. Otani, D. P. F. Hurley, H. Sun, and J. M. D. Coey, J. Appl. Phys. **69**, 5584 (1991).

[5] M. Katter, J. Wecker, C. Kuhrt, and L. Schultz, J. Magn. Magn. Mater. **114**, 35 (1992).

[6] M. Kubis, O. Gutfleisch, B. Gebel, K.-H. Müller, L. Schultz, and I. R. Harris, J. Alloys Compd. **283**, 296 (1999).

[7] O. Isnard, S. Miraglia, M. Guillot, D. Fruchart, and K. H. J. Buschow, J. Appl. Phys. **76**, 6035 (1994).
[8] F.-M. Yang, X.-W. Li, N. Tang, J.-L. Wang, Z.-H. Lu, T.-Y. Zhao, Q.-A. Li, J. P. Liu, and F. R. de Boer, J. Alloys Compd. **221**, 248 (1995).
[9] K. Koyama and H. Fujii, Phys. Rev. B **61**, 9475 (2000).
[10] A. Sippel, L. Jahn, M. Loewenhaupt, D. Eckert, P. Kerschl, A. Handstein, K.-H. Müller, M. Wolf, M. D. Kuz'min, L. Steinbeck, M. Richter, A. Teresiak, and R. Bewley, Phys. Rev. B **65**, 064408 (2002).
[11] O. Gutfleisch, J. Phys. D: Appl. Phys. **33**, R157 (2000).
[12] H. Kato, J. Shiomi, T. Koide, T. Iriyama, M. Yamada, and Y. Nakagawa, J. Alloys Compd. **222**, 62 (1995).
[13] G. Asti and F. Bolzoni, J. Magn. Magn. Mater. **20**, 29 (1980).
[14] K. P. Belov and A. N. Goryaga, Fiz. Met. Metalloved. **2**, 3 (1956).
[15] A. Arrott, Phys. Rev. **108**, 1394 (1957).
[16] M. D. Kuz'min, Phys. Rev. Lett. **94**, 107204 (2005).
[17] M. D. Kuz'min, D. Givord, and V. Skumryev, J. Appl. Phys. **107**, 113924 (2010).
[18] O. Isnard, S. Miraglia, M. Guillot, and D. Fruchart, J. Appl. Phys. **75**, 5988 (1994).
[19] *International Tables for Crystallography*, Vol. A, edited by T. Hahn (Springer, Dordrecht, 2005).
[20] M. T. Hutchings, Point-charge calculations of energy levels of magnetic ions in crystalline electric fields, in *Solid State Physics,* Vol. 16, edited by F. Seitz and D. Turnbull (Academic Press, New York, 1964), p. 227.
[21] A. V. Andreev, S. Yoshii, M. D. Kuz'min, F. R. de Boer, K. Kindo, and M. Hagiwara, J. Phys. Condens. Matter **21**, 146005 (2009).
[22] L. G. Onopriyenko, Phys. Met. Metallogr. **17**, 30 (1964).
[23] D. Melville, W. I. Khan, and S. Rinaldi, IEEE Trans. Magn. **12**, 1012 (1976).
[24] G. Asti, First-order magnetic processes, in *Handbook of Magnetic Materials*, Vol. 5, edited by E. P. Wohlfarth and K. H. J. Buschow (North-Holland, Amsterdam, 1990), Chap. 5.
[25] X. C. Kou, F. R. de Boer, R. Grössinger, G. Wiesinger, H. Suzuki, H. Kitazawa, T. Takamasu, and G. Kido, J. Magn. Magn. Mater. **177-181**, 1002 (1998).
[26] N. V. Kudrevatykh, A. V. Deryagin, A. A. Kazakov, V. A. Reymer, and V. N. Moskalev, Phys. Met. Metallogr. **45**, 38 (1978).
[27] R. Verhoef, J. J. M. Franse, F. R. de Boer, H. J. M Heerooms, B. Matthaei, and S. Sinnema, IEEE Trans. Magn. **24**, 1948 (1988).
[28] M. D. Kuz'min, Phys. Rev. B **46**, 8219 (1992).
[29] M. D. Kuz'min, J. Appl. Phys. **92**, 6693 (2002).
[30] N. Magnani, S. Carretta, E. Liviotti, and G. Amoretti, Phys. Rev. B **67**, 144411 (2003).
[31] F. Weitzer, K. Hiebl, and P. Rogl, J. Appl. Phys. **69**, 7215 (1991).
[32] E. R. Callen, J. Appl. Phys. **31**, S149 (1960).
[33] E. R. Callen and H. B. Callen, J. Phys. Chem. Solids **16**, 310 (1960).
[34] M. D. Kuz'min, K. P. Skokov, I. Radulov, C. A. Schwöbel, S. Foro, W. Donner, M. Werwiński, J. Rusz, E. Delczeg-Czirjak, and O. Gutfleisch, J. Appl. Phys. **118**, 053905 (2015).